



Update of Pheochromocytoma Syndromes: Genetics, Biochemical Evaluation, and Imaging

Rami Alrezk^{1,2,3†}, Andres Suarez^{1†}, Isabel Tena^{1,4†} and Karel Pacak^{1*}

¹ Section on Medical Neuroendocrinology, Eunice Kennedy Shriver National Institute of Child Health and Human Development, National Institutes of Health, Bethesda, MD, United States, ² National Institute of Diabetes and Digestive and Kidney Diseases, National Institutes of Health, Bethesda, MD, United States, ³ Cleveland Clinic, Adrenal Center, Endocrinology and Metabolism Institute, Cleveland, OH, United States, ⁴ Provincial Hospital, Castellon, Spain

OPEN ACCESS

Edited by:

Derek LeRoith,
Icahn School of Medicine at Mount
Sinai, United States

Reviewed by:

Luiz Eduardo Arondi Wildemberg,
Instituto Estadual do Cérebro Paulo
Niemeyer, Brazil
Agnese Barnabei,
Istituto Nazionale del Cancro Regina
Elena, Italy

*Correspondence:

Karel Pacak
karel@mail.nih.gov

†These authors share co-first
authorship

Specialty section:

This article was submitted to
Cancer Endocrinology,
a section of the journal
Frontiers in Endocrinology

Received: 24 April 2018

Accepted: 16 August 2018

Published: 27 November 2018

Citation:

Alrezk R, Suarez A, Tena I and
Pacak K (2018) Update of
Pheochromocytoma Syndromes:
Genetics, Biochemical Evaluation, and
Imaging. *Front. Endocrinol.* 9:515.
doi: 10.3389/fendo.2018.00515

Pheochromocytomas and paragangliomas (PCCs/PGLs) are rare commonly benign neuroendocrine tumors that share pathology features and clinical behavior in many cases. While PCCs are chromaffin-derived tumors that arise within the adrenal medulla, PGLs are neural-crest-derived tumors that originate at the extraadrenal paraganglia. Pheochromocytoma-paraganglioma (PPGL) syndromes are rapidly evolving entities in endocrinology and oncology. Discoveries over the last decade have significantly improved our understanding of the disease. These include the finding of new hereditary forms of PPGL and their associated susceptibility genes. Additionally, the availability of new functional imaging tools and advances in targeted radionuclide therapy have improved diagnostic accuracy and provided us with new therapeutic options. In this review article, we present the most recent advances in this field and provide an update of the biochemical classification that further reflects our understanding of the disease.

Keywords: pheochromocytoma, paraganglioma, genetics, biochemical classification, DOTATATE, PRRT

INTRODUCTION

According to the 2017 World Health Organization (WHO) classification of endocrine tumors, pheochromocytomas (PCCs) are tumors of the chromaffin cells that arise within the adrenal medulla (1), whereas paragangliomas (PGLs) are neural crest-derived neuroendocrine tumors (NETs) that can originate at any level of extra-adrenal paraganglia (from the skull base to the pelvic floor) (2). PCCs and PGLs arising from sympathetic paraganglia are characterized by catecholamine production whereas PGLs distributed along the parasympathetic chains of the head and neck (NHPGL) tend to be silent or pseudo-silent tumors (3–5).

The field of pheochromocytoma-paraganglioma (PPGL) is rapidly evolving. Many discoveries over the last decade have significantly improved our understanding of the disease. The identification of new hereditary forms of PPGL has led to the highest rate of germline susceptibility in cancer genetics at almost 40% (6, 7). In addition, other PPGL-related genes have been discovered and there are currently over 22 susceptibility genes identified. The genotype-phenotype correlation shown in many studies often dictates the clinical presentation of syndromic forms of the disease. These include associated biochemical profile, tumor location, malignant potential, aggressive clinical behavior, and overall prognosis. Furthermore, genetic identification provides valuable information for establishing a treatment plan and procures the rational for an appropriate guidance for follow-up surveillance.

The involvement of the Krebs cycle and the respiratory chain, mainly represented by the involvement of succinate dehydrogenase (SDH) in the etiology of PPGL, is perhaps the most important discovery in this area. Mutations of genes that encode any of the subunits A, B, C, or D or the complex assembly factor 2 (AF2) account for a group of overlapping yet distinct hereditary syndromes termed SDHx. These forms are considered the most common of all hereditary PPGL syndromes accounting for ~30% of them (6, 7). Over the past 6 years, ten new genes have been discovered. These new genes include hypoxia-inducible factor 2 alpha (*HIF2A*)—also known as endothelial PAS domain-containing protein 1 (*EPAS1*) (8, 9), fumarate hydratase (*FH*) (10), HRAS proto-oncogene (*H-RAS*) (11), prolyl hydroxylase 1 (*PHD1*)—also known as egl nine homolog 2 (*EGLN2*) (12), malate dehydrogenase 2 (*MDH2*) (13), chromatin remodeler *ATRX* (*ATRX*) (14, 15), H3 histone family member 3A (*H3F3A*) (15), cold-shock domain containing E1 (*CSDE1*) (15), coactivator 3 mastermind-like (*MAML3*) fusion genes [upstream binding transcription factor, RNA polymerase I] (*UBTF*)–*MAML3* (15), and iron regulatory protein 1 (*IRP1*) (16). Multiplicity regarding mosaicism underlines also in some syndromes (8, 9, 17, 18). Each of these genes mutations affects a specific metabolic pathway. As a result, The Cancer Genomic Atlas (TCGA) group

proposed a comprehensive system to classify PPGL-susceptibility genes into a molecular level. Based on genomic analysis, the system divides PPGL-related genes into four major clusters: a pseudohypoxia subtype (subdivided into tricarboxylic acid (TCA) cycle-dependent and *VHL/EPAS1*-dependent), a kinase-signaling subtype, a Wnt signaling subtype, and a cortical admixture subtype (**Figure 1**). These integrative efforts show that PPGL can be driven either by germline, somatic, or fusion genes mutations in 27, 39, and 7% of the cases, respectively (15).

GENETICS

Advances in genetics over the last decade have allowed the implementation of whole exome sequencing (WES) in developed countries as the new standard screening tool for genetic testing in patients with a suspected hereditary form of PPGL. However, the application of this technology is limited to specialized centers in developing countries. When available, the cost of testing is often a barrier for wide implementations of WES. Immunohistochemistry (IHC) is an alternative method in these cases, given its affordability and feasibility. It is used as screening tool where negative IHC for a gene can serve as an indirect indicator of the presence of a mutation in the gene of interest. This technique is especially useful in the context of suspected *SDHx* mutations (19–22). False-positive or false-negative results (19–22) are not uncommon, therefore, IHC should be interpreted with caution.

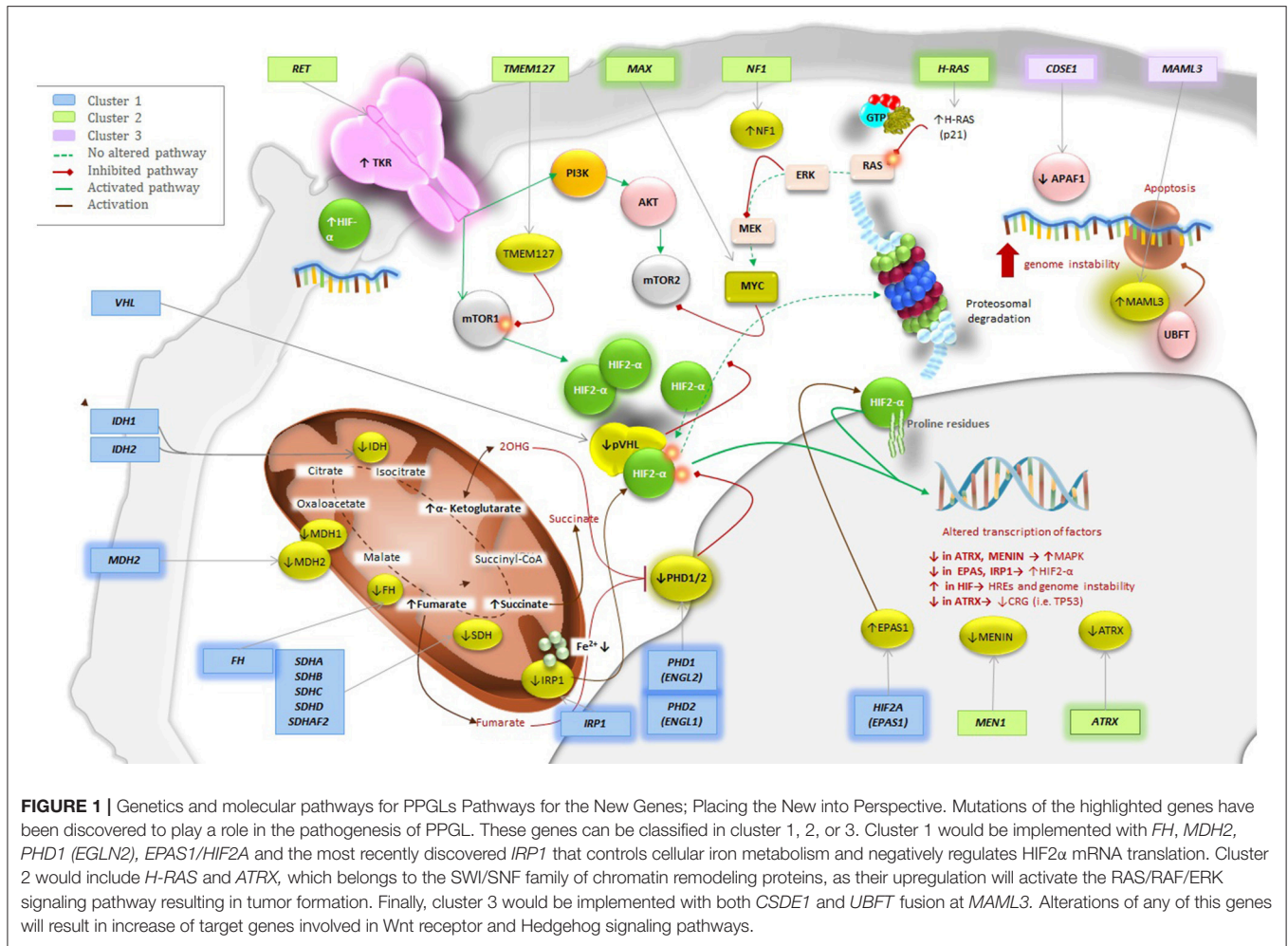
Integrative patient evaluation is essential as the clinical presentation, along with radiological and biochemical profile will guide clinicians toward the correct genetic diagnosis. This holds true when WES is not readily available. In these cases screening for specific gene or gene panels for a subgroup of susceptibility genes can be an alternative option. Therefore, we emphasize the importance of phenotype profile recognition (**Table 1, Figure 2**).

CLUSTER 1/PSEUDOHYPOXIA SUBTYPE

1A. TCA Cycle-Related *FH*:

FH is a tumor suppressor gene in the TCA cycle that encodes FH enzyme, which converts fumarate into malate (31). Deficiency in *FH* results in accumulation of the precursor metabolite fumarate, which shares structural similarities with succinate, leading to prolyl-hydroxylase (*PHD*) inactivation and HIF stabilization (32, 33). *FH* has an autosomal dominant inheritance with variable expressivity. Patients typically present with multiple cutaneous leiomyomatosis (*MCUL*). Leiomyomas are smooth muscle tumors that arise from the skin and uterus in these patients. When associated with renal cell cancer, this syndrome is referred to as hereditary leiomyomatosis and renal cell cancer (*HLRCC*) also known as Reed's syndrome (23). PPGL is a rare second manifestation of the syndrome and tends to be malignant and/or multiple and present with a predominant noradrenergic profile. To date, only few cases have been reported and both pathogenic germline and somatic mutations have been described (10, 34). Age of presentation varies widely from as

Abbreviations: 3-MT; 3-methoxytyramine; ¹⁸FDA, ¹⁸F-fluorodopamine; ¹⁸F-DOPA, ¹⁸F-fluorodopa; ¹⁸F-FDG, ¹⁸F-fluorodeoxyglucose; ⁶⁸Ga, ⁶⁸Galium; ⁹⁰Y, ⁹⁰Yttrium; ¹³¹I-MIBG, ¹³¹I-MIBG, metaiodobenzylguanidine; ¹¹¹In, ¹¹¹Indium; ¹⁷⁷Lu, ¹⁷⁷Lutetium; AFAP1, apoptosis protease activator protein 1; AKT, serine/threonine kinase; *ATRX*, chromatin remodeler *ATRX*; CT, computerized tomography; CRG, growth regulatory factors; *CSDE1*, cold-shock domain containing E1; CVD, cyclophosphamide, vincristine and dacarbazine; DA, dopamine; DIPG, diffuse intrinsic pontine glioma; DOTA, tetraazacyclododecanetetraacetic acid; DOTATATE, DOTA-Tyr3-octreotate; DS, direct sequencing; E, epinephrine; *EGLN1/2*, egl nine homolog 1 and 2; *EPAS1*, PAS domain-containing protein 1; EPO erythropoietin; EpoR, erythropoietin receptor; ERK, extracellular mitogen-activated protein kinase 1; FDA, food and drug administration; *FH*, fumarate hydratase; HNPGL, head and neck paraganglioma; GTC, giant cell tumor of the bone; GTP, guanosine-5'-triphosphate; *H3F3A*, H3 histone family member 3A; HNPGL head and neck PGL; *HIF2α* hypoxia-inducible factor 2 alpha; *HIF2A*, hypoxia-inducible factor 2 alpha; H LPC, high-performance liquid chromatography; HLRCC, leiomyomatosis and renal cell cancer; *H-RAS*, HRAS proto-oncogene; *IDH1/2*, isocitrate dehydrogenase 1 and 2; IHC, immunohistochemistry; *IRP1* iron regulatory protein; *MCUL*, multiple cutaneous leiomyomatosis; *MDH1/2*, malate dehydrogenase type 1 and 2, *MAML3*; coactivator 3 mastermind-like; MAPK, mitogen-activated protein kinase; MAX, myc-associated factor X gene; Men1, multiple endocrine neoplasia 1; LC-MS, liquid chromatography tandem-mass spectrometry; MEK, mitogen-activated protein kinase; MLPA, multiplex ligation-dependent probe amplification; MN, metanephrine; MRI, magnetic resonance imaging; mRNA, messenger ribonucleic acid; mTOR, mammalian target of rapamycin; NE norepinephrine (NE); NETs neuroendocrine tumors; NF1, neurofibromin 1; NIH, National Institutes of Health; NMN, normetanephrine; NET, neuroendocrine tumor; PCC, pheochromocytoma; PET, positron emission tomography; PGLs, paraganglioma; *PHD1/2*, prolyl hydroxylase 1 and 2; PI3K, phosphatidylinositol-3-kinase; PPGL, pheochromocytoma-paraganglioma; PRRT, peptide receptor radionuclide therapy; RF, radiofrequency; SDH, succinate dehydrogenase subunits A/B/C/D; SDHAF2, succinate dehydrogenase complex assembly factor 2; SPECT, single photon emission computed tomography; SSA, somatostatin analogs; SSTR, somatostatin receptor; TCA, tricarboxylic acid, TA, thermoablation; TCGA, The Cancer Genomic Atlas, TFG, transcription factors genes; TMEM127, transmembrane protein 127; TMZ, temozolomide; TSG, tumor suppressor gene; *UBTF*, upstream binding transcription factor; *VHL*, von Hippel Lindau; WES, whole exome sequencing; WHO, World Health Organization.



young as 6- to 70-years-old. More recently, a study of a cohort reported by the National Institutes of Health (NIH) revealed co-secreting dopamine (DA) tumors in some *FH* mutated patients (24).

1B. *VHL*/*EPAS1*-Related *EPAS1*/*HIF2A*:

EPAS1 (*HIF2A*) is an oncogene that encodes the EPAS1; a transcription factor related to oxygen level responses (35). In 2012, Zhuang et al. were the first to identify a gain-of-function somatic mutation in exon 12 of *EPAS1* (G1588A and C1589T) in patients with PPGLs. These mutations caused defects on the proline residues at the hydroxylation site of *HIF2α* leading to its reduced degradation and stabilization (8, 9). Since then, other cases of PPGL with polycythemia have been reported. Among them, somatic mutations of *HIF2A* at exon 12 are responsible in most cases of the disease, and only one case was caused by germline mutation of *HIF2A* at exon 9 (36). Furthermore, both germline mosaicism/somatic mutations have been described in additional studies (18, 36). Somatic *HIF2A*-related PPGL affects predominantly females and patients typically presents with PPGL, somatostatinoma and polycythemia (Pacak-Zhuang

syndrome) (8). However, penetrance can vary from patient to patient and incomplete forms of the disease have been reported. In particular, the presence of somatostatinoma has not been described in males yet. PPGLs in these patients are often multiple or recurrent with elevated norepinephrine (NE), normetanephrine (NMN), DA, and erythropoietin (EPO) and once third of the patients present with metastatic disease (37). Also, ~70% of the patients have been found to have ocular abnormalities with bilateral dilated capillaries and fibrosis overlying the optic disc being the most common findings. Therefore, an early referral to an ophthalmologist acquainted with the retinal findings of this syndrome is strongly recommended (38). Surgery of the PPGL, often results in an improvement of *HIF2A*-induced polycythemia but treatment of the disease still requires intermittent phlebotomies, and control blood pressure to prevent complications resulting from polycythemia.

Cluster 2/Kinase Signaling Group *H-RAS*:

Located on chromosome 11p.15.5, *H-RAS* is a proto-oncogene that, encodes H-RAS factor (also known as transforming

TABLE 1 | Genetics and clinical profile for the newly discovered forms of PPGLs.

Gene	Syndrome	Biochemical profile	Date of discovery	Gene role	Clinical presentation	Gene type	Cluster	Inheritance	References
<i>FH</i>	HLRCC	Noradrenergic	2012	TSG; encodes FH that catalyzes the reversible hydration of fumarate to L-malate in the TCA cycle. Increase in fumarate leads to stabilization of HIF	Multifocal, metastatic, associated with RCC and leiomyomatosis	G	1	AD	(10, 23–25)
<i>HIF2A</i> or <i>EPAS1</i>	Pacak-Zhuang	Noradrenergic	2012	Oncogene; encodes EPAS1; transcription factor related to oxygen level responses and activated in hypoxic conditions	Triad of PPGLs, polycythemia, and somatostatinoma. Ocular abnormalities occur in 70%	S/M	1	N/A	(8, 9, 24, 26)
<i>H-RAS</i>	Adrenergic	Adrenergic	2013	Proto-oncogene; encodes H-RAS (P21), that once bound to GTP, activates the RAS/RAF/ERK signaling pathway leading to cell proliferation	Unilateral PCC, sporadic, benign	S	2	N/A	(11, 27)
<i>H3F3A</i>	Unknown	Unknown	2013	Encodes the histone H3.3 protein, responsible for chromatin regulation	Giant cell tumors of the bones (GCT), PCCs, bladder and periaortic PPGL	S	*	N/A	(28)
<i>EGLN2 (PHD1)</i>	Noradrenergic	Noradrenergic	2015	TSG; encodes PHD1, enzyme which in normal oxygen conditions, hydroxylates specific proline residues of the HIF- α subunits for posterior degradation in the proteasome	Polycythemia associated with recurrent PPGLs, and normal or mild elevated EPO	G	1	**	(12)
<i>MDH2</i>	Noradrenergic	Noradrenergic	2015	TSG; encodes MDH2 that catalyzes the reversible oxidation of malate to oxaloacetate in the TCA cycle.	Multiple PGLs	G	1	AD	(13)
<i>ATRX</i>	ATRX	Noradrenergic	2015	Increase in malate, fumarate and succinate leads to stabilization of HIF Encodes the transcriptional regulator ATRX	Clinically more aggressive and metastatic PGL	S	*	N/A	(29)
<i>CSDE1</i>	Adrenergic	Adrenergic	2016	Tumor suppressor gene. Involved in normal development through messenger RNA stability internal initiation of translation, and cell-type-specific apoptosis.	Sporadic, metastatic, recurrent PPGL	S	*	N/A	(15)
<i>UBTF-MAML3 fusion</i>	Adrenergic	Adrenergic	2016	Oncogene. In PPGLs, unique hypomethylation profile mRNA overexpression of target gene involved in Wnt receptor and Hedgehog signaling pathways	Sporadic, recurrent PGL. New prognostic factor of poor outcome	F	3	N/A	(15)
<i>IRP1</i>	IRP1	Noradrenergic	2017	TSG; encodes IRP1, that controls cellular iron metabolism and negatively regulates HIF2 α mRNA translation under iron-deficient conditions. Deficiency of IRP1 protein increases HIF2 α	Sporadic, adrenal PCC	S	1	N/A	(30)

S, somatic; G, germline; M, mosaicism; F, fusion; PCC, renal cell carcinoma; HLRCC, hereditary leiomyomatosis and renal cell cancer; PCC, pheochromocytoma; PPGL, pheochromocytoma-paraganglioma; TSG, tumor suppressor gene; GCT, giant cell tumor.
 N/A, Not Applicable in the setting of somatic mutations.
 AD, Autosomal Dominant.
 *Not classified by clusters, **Unknown.

protein p21). H-RAS, once bound to guanosine-5'-triphosphate (GTP), activates the RAS/RAF/ERK signaling pathway that will ultimately result in cell proliferation (27). Pathogenic mutations in *H-RAS* were firstly identified in 2013. WES of tumor DNA in four cases with phenotype suggesting an underlying pathogenic genetic variant revealed the presence of 2 hotspot mutations in *H-RAS* (G13R and Q61K) in two of them. In all four samples, known susceptibility genes had been previously excluded (11). All four cases were male patients with unilateral, sporadic/benign tumors (three PCCs and one abdominal PGL), along with elevation in plasma catecholamines. Further validation in a cohort of 58 additional samples obtained showed an accumulated frequency of 6.9% (4/58) of missense somatic mutations in *H-RAS*: G13R ($n = 1$), Q61K ($n = 1$), and Q61R ($n = 2$) (11).

Cluster 3/WNT Signaling Group CSDE1:

Formerly known as upstream of N-ras (*UNR*), *CSDE1* is a tumor suppressor gene located at chromosome 1p13.2 that encodes CSDE1 factor, which is mainly involved in development and has several functions including messenger RNA stability, internal initiation of translation, cell-type-specific apoptosis and neuronal differentiation (39, 40). The association of *CSDE1* to PPGL was recently described by TCGA group in a cohort study of 176 PPGL patients, in which four were found to have a somatic mutation—two frameshift, and two splice-site—, in *CSDE1* (15). Underexpression of *CSDE1* has been reported in several tumors (41). Mutations in this gene result in downregulation of the apoptosis protease activator protein 1 (*APAF1*), which controls apoptosis in PCC cells under normal conditions (42, 43). Clinically, patients presented with sporadic cases, and some of them with recurrence or metastatic disease proposing a more aggressive form of PPGLs (15).

UBTF-MAML3 Fusion:

MAML3 (4q31.1) is an oncogene that had been previously associated with other tumor types (44, 45). On the other hand, *UBTF* (17q21.31), encodes UBTF required for the expression of rRNA subunits (46). The association of the fusion with PPGL was identified by TCGA group in 2017 when analysis from RNA sequencing of the same cohort mentioned above revealed that ten tumors (eight primary, and two primary-metastatic) were positive for a *MAML3* fusion gene. Patients presented with a unique and expansive hypomethylation profile that was correlated with mRNA overexpression of target genes involved in developmental pathways, such as Wnt receptor signaling and Hedgehog signaling, that were significantly overexpressed including miR-375, β -catenin, *DVL3*, and *GSK3* (15). *MAML3*-related PPGLs had the highest Ki-67 index expression, and some patients presented with aggressive disease (15). Finding *UBTF-MAML3* fusion predicts a poor prognosis, as compared with other syndromic forms of PPGL (15).

PROPOSED CLASSIFICATION FOR NEW GENES ACCORDING TO TCGA

Three additional genes were not included in the molecular classification done by TCGA (15). However, based on their signaling pathways, we believe that all three should be included as part of the cluster 1 or pseudohypoxia signaling group for future updates. While *MDH2* is a part of the TCA cycle, both *PHD1* (*EGLN2*) and *IRP1* belong to the *VHL/EPAS1*-related subtype (Figure 1) and have been very recently described.

MDH2:

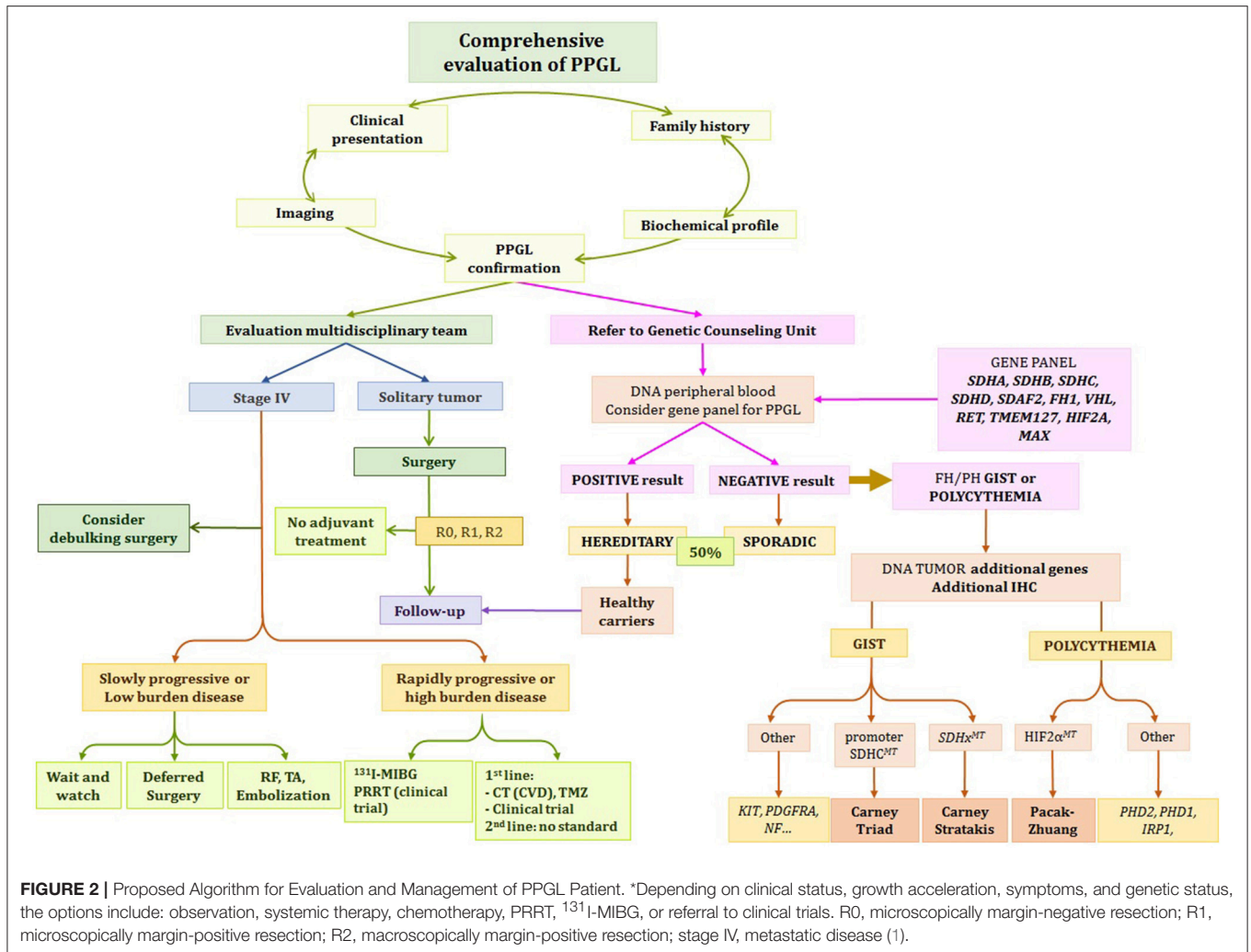
MDH2 encodes the MDH2 enzyme, which catalyzes the reversible oxidation of malate to oxaloacetate in the TCA cycle. Deficiency of MDH2 has shown to lead to the accumulation of malate, fumarate, and succinate on *Drosophila* models (47). Thus, *MDH2* should be classified as a cluster 1-TCA cycle-related gene. In 2015, Cascon et al. were the first to report a case with a germline mutation in *MDH2*: a male patient diagnosed with multiple PGLs (13). Later, five asymptomatic relatives were tested, and two were found to be positive. Subsequent updates showed elevation of NE and the presence of a hypermethylator phenotype similar to *SDHx*-related PPGLs (48). Interestingly, no malate accumulation was found on tumor cells, but a high fumarate/succinate ratio was observed (13).

PHD1 (EGLN2):

PHD1 (*EGLN2*) encodes PHD1 enzyme, which in normal oxygen conditions hydroxylates specific proline residues of the HIF- α subunits for their subsequent degradation by proteasome. Deficiency of this enzyme prevents degradation of HIF- α and resulting in HIF stabilization leading to a global activation of signaling pathways that lead to tumorigenesis (49). *PHD1* should therefore be classified as cluster 1-*VHL/EPAS1*-related gene. In 2008, Ladroue et al. were the first to describe the association of mutations in *PHD2* with polycythemia and PPGLs (50). Seven years later, Yang et al. reported the first mutation in *PHD1* (*EGLN2*), found to be associated with PPGL, along with an additional case with *PHD2* (*EGLN1*) germline mutation. These two patients presented with multiple recurrent PPGL, polycythemia with normal or mildly elevated EPO, and were negative for *HIF2A* mutation. Both patients presented with catecholamine related symptoms including: headaches, episodic chest pain, anxiety, and hypertension. Both cases revealed a noradrenergic profile. In the patient with the mutation in *PHD1* (*EGLN2*), sensitivity of erythroid progenitors to EPO and erythropoietin receptor (EpoR) activity were inappropriately increased and resulted in polycythemia with no or mild increase in EPO levels with increased EpoR expression (12).

IRP1:

IRP1 is a tumor suppression gene that encodes IRP1, a bi-functional protein that controls cellular iron metabolism and negatively regulates HIF2 α mRNA translation under iron-deficient conditions (51, 52). Thus, deficiency of IRP1 increases



HIF2 α by dissociating sequences of HIF2 α mRNA from iron-responsive element and suppressing protein translation. Activation of HIF-2 α leads to an increase of transcription of EPO and EpoR. Recently, *IRP1* association with PCC was reported by Pang et al. in a patient with a medical history of polycythemia vera with a proven *JAK2* mutation, hypertension, diaphoresis, and abdominal pain that led to the diagnosis of PCC years later. An investigational gene panel consisting of 54 tumor-associated genes was negative for patient's peripheral blood DNA. Subsequent tumor DNA sequencing revealed a somatic, loss of function mutation in *IRP1* located on exon 3 splicing site (16).

Driver Mutation Gene With Unknown Classification

H3F3A

Located on chromosome 1, *H3F3A* encodes the histone H3.3 protein (53). Histones are responsible for nucleosome formation, and as a chromatin regulator, mutations of this gene will affect DNA methylation, chromatin remodeling, or nucleosome positioning (54). Defects in *H3F3A* have been linked with diffuse

intrinsic pontine glioma (DIPG) (55, 56), chondroblastoma, and giant cell tumor of the bone (GCT) (57). Association with PPGL was initially reported in 2013 as a case report (58). Three years later, in 2016, Toledo et al. analyzed 43 samples of 41 patients using exome or transcriptome sequencing and detected a postzygotic *H3F3A* mutation in three tumors from one patient with a history of recurrent GCT. This patient presented with bilateral PCCs and developed bladder and several periaortic PGLs later. Family history of PPGL was absent. Further analysis showed that this mutation was identical to an oncogenic driver of sporadic GCT (c.103 G > T, p.G34W) (57, 58). Furthermore, additional variants in other chromatin remodeling genes (*KMT2B*, *EZH2*, *SETD2*, *ATRX*, *JMJD1C*, *KDM2B*) were reported in this study (28). Additionally, two kinase receptor-encoding genes (*MERTK*, *MET*) were found (28). Also, the investigators detected a somatic mutation in the main hotspot residue of the fibroblast growth factor receptor 1 gene (28), which is known to play a role in other cancers, such as glioblastomas (59). Further studies are needed to clarify the role of these genes in the pathogenesis of PPGL.

DISEASE MODIFYING GENE

ATR_X

Located on the X chromosome, *ATR_X* encodes the transcriptional regulator ATRX, which belongs to the SWI/SNF family of chromatin remodeling proteins. ATRX plays a role in the histone deposition in telomeres, chromosome segregation in the cell cycle and transcription regulation (60–62). Germline mutations in *ATR_X* have been reported as a cause of X-linked alpha thalassemia mental retardation syndrome (ATR_X syndrome) (63). In 2015, using WES, Fishbein et al. reported somatic *ATR_X* mutations in two *SDHB*-related frozen tumors. They found somatic *ATR_X* mutations in 12.6% of the samples, along with an alternative lengthening of telomeres seen on fluorescence *in situ* hybridization (FISH) and presenting with more aggressive disease (29). Later, the first case of an *ATR_X* driver mutation was reported in a patient with a metastatic composite PCC-PGL, clinically with anemia, weight loss, and hepatic metastases. WES showed a somatic loss of function on the *ATR_X* gene, along with downregulation of genes involved in the neuronal development and homeostasis (*NLGN4*, *CD99*, and *CSF2RA*) and upregulation of *Drosha* gene related with RNA processing and alternative lengthening of telomeres (14). Somatic mutations have been reported in association with co-existing mutations in the isocitrate dehydrogenase 1 and 2 (*IDH 1/2*) genes in both adult and pediatric patients with astrocytic tumors (64). In addition, *ATR_X* may play a driver mutation role for sporadic PPGL (14) and truncated *ATR_X* could potentially play a synergistic role with *SDHx* in tumor initiation and might be a predisposition for a more aggressive disease (15).

Biochemical Evaluation

Biochemical evaluation has made tremendous strides forward since the 1950's when colorimetric assays were first implemented, and later replaced with the more accurate high-performance liquid chromatography (HPLC) in the 1980s. Currently, liquid chromatography tandem-mass spectrometry (LC-MS) has become the new gold standard due to its accuracy and reproducibility. A value three times the upper range of normal is a positive result. However, some patients present with pseudo-silent PPGL and high tumor burden resulting in a late diagnosis. Therefore, any values above the normal range should be carefully considered as positive in the setting of prospective screening in hereditary forms of the disease, given early proactive surveillance has made pre-detection of tumors very possible.

Besides screening and diagnoses, biochemical phenotype of the tumor is a useful tool for PPGL syndromic assessment. PPGLs can be classified according to their biochemical profile. This classification allows the establishment of an algorithm and addresses specific causative genes. Here, we present an update of the different PPGL-related biochemical phenotypes.

A- Truly biochemically silent phenotype: Often associated with *SDHx* syndromes, truly silent PPGLs are mostly located in

the head and neck area (HNPGL). Among HNPGL, carotid body tumors are the most frequent (65), followed by glomus vagale, jugulotympanic, and laryngeal PGLs.

B- Biochemically pseudo-silent phenotype: In this category, PPGLs present with levels of catecholamines and metanephrines that can be “normal” or “near-normal” in a misleading way. This category should be distinguished from group A since PPGLs in this category are indeed catecholamine-producing tumors. However, detection of elevated metanephrine and normetanephrine falls below the limit of detection due to either low tumor burden or catecholamine production fluctuations. This usually happen in patients with very small (less than 5–7 mm) PPGLs.

C- Noradrenergic phenotype: Characterized by increased levels of NE/NMN (66, 67), noradrenergic PPGLs are commonly located outside the adrenals (66, 67), NE acts on both α (1 and 2) and β (1, 2, and 3) adrenoreceptors with predominant effect on α . These patients present less frequently with paroxysmal symptomatology. Sustained hypertension and tachycardia are the most common symptoms. However, hypertensive crisis, myocardial infarction, lethal tachyarrhythmia, and acute intramural hemorrhage have been reported (68, 69). This phenotype is commonly seen in the cluster 1/ pseudohypoxia group (15), including both *VHL* and *SDHx* mutations (70).

D- Adrenergic phenotype: These PPGLs are characterized by either purely elevated epinephrine (E)/metanephrine (MN) (66), or in both E/MN and NE/NMN. This phenotype can be accurately identified when the plasma level of free MN is greater than 10% of the sum of NMN and MN (66). Adrenergic PPGLs are often located in the adrenal gland (67). Epinephrine represents a higher level of cellular differentiation of adrenal PPGL when compared with tumors derived from paraganglia (71, 72). Epinephrine activates α -1 and α -2 adrenoreceptors with a higher affinity compared to NE (73) but also affects β -2 adrenoreceptors. Paroxysmal symptomatology due to a rapid metabolism (74) has been related to the concomitant use of medications like histamine, tricyclic antidepressants (TCA), anesthetics, and tyramine-rich food (75). In many cases these patients are found to have hyperglycemia and hyperlipidemia secondary to the stimulus of lipolysis, glycogenolysis, and gluconeogenesis (68). This phenotype is commonly seen in the cluster 2/kinase signaling group (15).

E- Dopaminergic phenotype: These PPGLs are characterized by high levels of DA/3-methoxytyramine (3-MT) with normal or near-normal levels of E/MN and NE/NMN (75, 76). Tumors are commonly extra-adrenal and primarily located in the head and neck region (77, 78). Patients can be either asymptomatic or have atypical symptoms like abdominal pain, diarrhea, nausea/vomiting, hypotension, and weight loss. These symptoms are most likely related to dopamine receptor stimulation on the smooth muscle (79), gastrointestinal tract (80), and central nervous system (81). This subset of patients has been traditionally classified as biochemically “silent”. Elevated levels of DA/3MT together with NE have been reported in approximately 65% of patients with *SDHx* mutations, especially in *SDHB* (76, 82).

Experts Recommendations and Meta-Analysis

The Endocrine Society 2014 guidelines recommend initial screening with either plasma or urine fractionated MN/NMN, with the consensus that values three to four times higher than the upper reference limit are almost always diagnostic for PPGLs (83). A recent meta-analysis done by Därr et al., compared the accuracy of plasma and urine metanephrines in 1,039 patients with PPGL. The study also compared immunoassay methods—HPLC and LC-MS—and differences between supine vs. seated position during sampling. Results in terms of sensitivity/specificity/accuracy showed that supine sampling was more sensitive in tumor detection (95 vs. 89% [$p < 0.02$]). Furthermore, the supine position has a higher specificity than 24-h urine samples (95 vs. 90% [$p < 0.03$]) and the highest accuracy (95%), especially when measured with HPLC and LC-MS over immunoassay (84) as LC-MS eliminates drug interference providing more accurate results.

When evaluating pediatric patients with PPGL, considerations for age-adjusted reference values are crucial to determine the tests positivity. Higher limits for E/MN along with lower limits for NE/NMN were seen in children when compared with adults (85). Finally, we wish to note that LC-MS is not widely available in all countries. Cost of technology itself as well as a lack of trained staff stand as barriers to full implementations of LC-MS (86).

Imaging

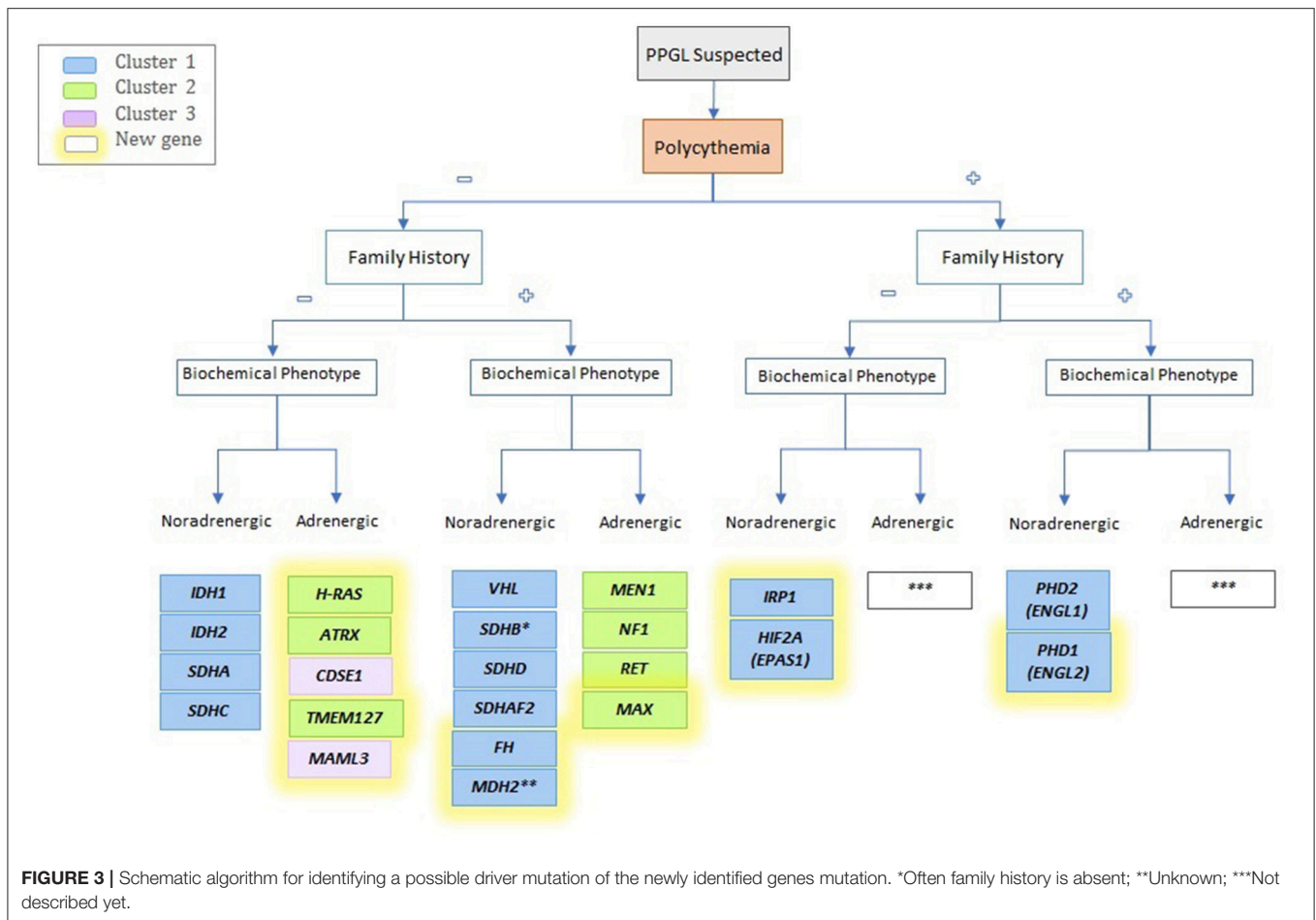
The latest Endocrine Society Guidelines (83) emphasize that consideration for any imaging modality in PPGLs requires prior positive biochemical evidence of disease except for the presence of personal or family history of HNPGL related or not to a hereditary form of the disease. For a general work-up, computed tomography (CT) is recommended as the anatomic imaging modality of choice due to its excellent spatial resolution. Magnetic resonance imaging (MRI) is recommended for children, pregnant women, or patients with HNPGL or metastatic disease. Regarding functional imaging the panel of experts suggests the use of ^{123}I -metaiodobenzylguanidine (MIBG) scintigraphy in patients with metastatic disease when treatment with radiotherapy using ^{131}I -MIBG is considered or when the risk of metastasis or recurrence of the disease is high based on tumor size. However, if metastatic disease is confirmed, the use of ^{18}F -fluorodeoxyglucose (^{18}F -FDG) positron emission tomography hybridized with CT (PET/CT) is preferred (83).

We believe PPGL is a disease “born to be filmed” as the availability of high-value modalities for imaging provides a versatile algorithm to evaluate the different scenarios of the disease: in the initial evaluation setting, in treatment planification, and for tumor response assessment. This is due to the expression of various transporters and receptors in the surface of PPGL cells. Receptors that can be exploited for imaging include the NE transporter, glucose transporter (GLUT), amino acid transporter, and somatostatin receptor (SSTR) (87, 88). Currently, there are three types of PET/CT radiopharmaceuticals that exert their actions through these receptors: ^{18}F -FDG, ^{18}F -fluorodopa (^{18}F -FDOPA), and ^{68}Ga Galium

(^{68}Ga)- tetraazacyclododecanetetraacetic acid (DOTA) analogs (89–91). Functional imaging using PET/CT has proven to be superior to ^{123}I -MIBG SPECT not only for the higher detection, sensitivity, localization, and resolution, but also for reducing indeterminate or equivocal findings by about 20 to 40% (92). Among these modalities, ^{68}Ga -DOTA-Tyr3-octreotate (DOTATATE) PET/CT has emerged as the preferred modality in NETs in general. This is due to the high affinity of the radiolabeled compound for the SSTR type 2 (SSTR₂) (93) that can more accurately predict a tumor response to treatment to radiolabeled somatostatin analogs in patients with avidity for the tracer. In terms of tumor detection, ^{68}Ga -DOTATATE PET/CT has proven to be exceptional with a 98.6% overall detection rate in patients with *SDHB* metastatic PPGL, superior to anatomic imaging (CT/MRI), and other functional scans (^{18}F -FDG, ^{18}F -FDOPA, and ^{18}F -FDA PET/CT) (94). Similar results were also observed in sporadic cases with a sensitivity of 97.6% (89, 95) and in patients with HNPGL (96). Regarding specific mutations, ^{68}Ga -DOTATATE PET/CT resulted inferior in the evaluation of patients with polycythemia/PPGL— including both *HIF2A* and *PHD1*-related tumors—(97), *FH* or *MAX* mutations. In these patients— polycythemia associated to PPGL—, the combination of ^{18}F -FDOPA PET/CT and ^{18}F -FDA PET/CT resulted superior with a lesion-base detection rate of ~98%, vs. 35.3% for the ^{68}Ga -DOTATATE PET/CT group (95% CI, 25.0–47.2%) (97). With respect to *FH*-related tumors, in a patient reported ^{68}Ga -DOTATATE PET/CT showed an overall detection of 66% when compared to ^{18}F -FDOPA PET/CT (98). In reference to *MAX*-related PCCs, in a recent study evaluating six patients, ^{68}Ga -DOTATATE accuracy was lower than ^{18}F -DOPA PET/CT (99). Based on these studies authors suggest allocating both ^{18}F -FDOPA and ^{18}F -FDA PET/CT in the diagnostic algorithm of polycythemia/PPGL patients and designate ^{18}F -FDOPA PET/CT as first functional imaging modality of choice in the diagnoses and follow-up of both *MAX* and *FH*-related patients. If the availability of ^{18}F -FDA and ^{18}F -FDOPA PET/CT is limited, use of other imaging modalities like ^{123}I -MIBG single-photon emission CT (SPECT) is recommended.

Regarding the pediatric population, ^{68}Ga -DOTATATE PET/CT has shown to be superior in a cohort of nine children with *SDHx*-related PPGL with a detection rate of 98.4% when compared to ^{18}F -FDG PET/CT (100). However, these results are intriguing as another study reported that the sensitivity of ^{68}Ga -DOTATATE PET/CT is lower for abdominal lesions in children, with a detection rate of 66.7% (100, 101), warranting additional larger studies in this population. Thus, the use of more than one functional imaging modality is recommended in the pediatric group and the use of both ^{68}Ga -DOTATATE and ^{18}F -FDG PET/CT is highly recommended in children with small lesions, when there is a high likelihood of metastatic disease and in those patients with *SDHx* mutations.

The utility of functional imaging using somatostatin analogs, was recently extended and exploited to open new doors for targeted radiotherapy using the both ^{177}Lu (^{177}Lu) or ^{90}Y (^{90}Y). The ‘so-called’ peptide receptor radionuclide therapy (PRRT) has shown to a very effective therapeutic option in patients with advanced midgut NETs in a phase 3 clinical



trial called NETTER-1 published in 2017 (102). As a result, ^{177}Lu -DOTATATE (Lutathera[®]) has been recently approved by the food and drug administration (FDA) for the treatment of advanced midgut NETs. Applications of PRRT in PPGL have been assessed also in two small cohorts of patients with mediastinal or HNPGL (103) and with inoperable HNPGL (104), with promising outcomes in terms of tumor response and control of symptoms. A higher number of patients ($N = 20$) received four cycles of Lutathera[®] with encouraging results in terms of control of symptoms (decreased medication requirements), circulating chromogranin A, tumor response and control of disease with a median progression-free survival (PFS) of 29 months (105). When comparing PRRT with ^{131}I -MIBG in 22 patients with metastatic/progressive PPGL, PRRT showed increased PFS and tumor response rate, as well as increased event-free and overall survival (OS) (106). An ongoing prospective clinical trial at the NIH evaluating PRRT for progressive PPGL will provide definite answers regarding the utility and safety of PRRT in PPGL (NCT03206060).

The role of SSTR antagonists appears to be promising in the field of NETs. SSTR antagonists recognize more binding sites on SSTRs allowing better tumor visualization (107). Their clinical utility in functional imaging was first demonstrated in 2011 (108). A second-generation of SSTR₂ antagonists that include

DOTA-JR11 showed higher tumor uptake when combined with ^{68}Ga -DOTA (1.3 times), or ^{68}Ga -NODAGA (1.7 times) as compared with DOTA analogs (109). In the preclinical setting, DOTA-JR11 was superior to ^{177}Lu in H69 cell lines, and *in vivo* therapy experiments achieved a higher uptake, median survival rate, and a longer delay in tumor growth (110). Regarding pharmacokinetics and dosimetry, DOTA-JR11 showed very promising results when tested in human embryonic kidney cells with a higher uptake and longer tumor residence time. With an escalating dose DOTA-JR11 demonstrated an improved safety profile and the potential decrease toxicity (111). In *in vitro* studies including both NETs and non-NETs, DOTA-JR11 showed a higher affinity for SSTRs when compared to the SSTR₂ agonist ^{125}I -Tyr3-octreotide in NETs (2.5 to 40 times). Interestingly, the group of other non-NETs tumors— such as breast cancer, renal cell carcinoma, medullary thyroid cancer, and non-Hodgkin lymphoma—, was also targeted with high affinity, potentially opening a new door for exploring this modality in tumors where typically SSTR have played little role, if any (112). Currently, an ongoing clinical trial for metastatic and unresectable progressive, well-differentiated carcinoid is trying to elucidate the role of SSTR antagonist DOTA-JR11 both in diagnostic and therapeutic settings (NCT02609737).

CONCLUSION

In this article, we presented some of the latest advances in the rapidly evolving field of PPGL and we focused on genetic, biochemical and imaging discoveries over the last 6 years. In addition, we proposed an updated biochemical classification and provided a novel algorithm for identifying newly diagnosed PPGL (Figure 3). Ten new susceptibility genes related to PPGL have been described in the last 10 years, including new germline as well as somatic mutations. The last can be presented as mosaicisms and result in syndromic forms of the disease. Also, functional imaging modalities continue to improve, and lesion-base detection studies are more reliable and accurate. The wide availability of ^{68}Ga -DOTATATE PET/CT following the approval of the radiopharmaceutical compound by the FDA, is revolutionizing the way we diagnose not only PPGLs but also NETs in general. The expression of SSTR² on PPGL cells has allowed the exploitation of this modality as a therapeutic option in these patients using Lutathera[®], which was recently approved for use in midgut NETs. Current ongoing clinical trials in PPGL will determine safety, tolerability profile, and also efficacy in terms of clinical benefit and control of disease. Hopefully the availability of these diagnostic modalities will be more implemented in developing countries in the future. The expense associated with these technologies stands as a barrier; therefore, referral to centers of excellence that specialize in PPGL is warranted and highly advisable as implementation of theranostics into an algorithm is required for establishing different therapeutic options.

REFERENCES

- Tischler ASKRR, Gill A, Kawashima A, Kimura N, Komminoth P, Papathomas TG, et al. Tumours of the adrenal medulla and extra-adrenal paraganglia. In: Lloyd RV, Osamura RY, Klöppel G, Rosai J, editors. *WHO Classification of Tumours of Endocrine Organs 4th Edition*. Lyon: International Agency for Research on Cancer (IARC) (2017). pp. 179–207.
- Whalen RK, Althausen AF, Daniels GH. Extra-adrenal pheochromocytoma. *J Urol*. (1992) 147:1–10. doi: 10.1016/S0022-5347(17)37119-7
- Kimura N, Miura Y, Nagatsu I, Nagura H. Catecholamine synthesizing enzymes in 70 cases of functioning and non-functioning pheochromocytoma and extra-adrenal paraganglioma. *Virchows Arch A Pathol Anat Histopathol*. (1992) 421:25–32. doi: 10.1007/BF01607135
- Mena J, Bowen JC, Hollier LH. Metachronous bilateral nonfunctional intercarotid paraganglioma (carotid body tumor) and functional retroperitoneal paraganglioma: report of a case and review of the literature. *Surgery* (1993) 114:107–11.
- van Duinen N, Steenvoorden D, Kema IP, Jansen JC, Vriends AH, Bayley JP, et al. Increased urinary excretion of 3-methoxytyramine in patients with head and neck paragangliomas. *J Clin Endocrinol Metab*. (2010) 95:209–14. doi: 10.1210/jc.2009-1632
- Castro-Vega LJ, Letouzé E, Burnichon N, Buffet A, Disderot PH, Khalifa E, et al. Multi-omics analysis defines core genomic alterations in pheochromocytomas and paragangliomas. *Nat Commun*. (2015) 6:6044. doi: 10.1038/ncomms7044
- Jochmanova I, Pacak K. Genomic landscape of pheochromocytoma and paraganglioma. *Trends Cancer* (2018) 4:6–9. doi: 10.1016/j.trecan.2017.11.001

We are now entering a new and exciting era for PPGL that will allow us to advance one step further toward personalized medicine, making precision medicine for PPGL a step closer (Figure 2).

AUTHOR CONTRIBUTIONS

RA: writing and editing MS, creating Table 1 and Figure 3, proposing the idea of an update in the biochemical classification; AS: writing MS; IT: writing, editing and reviewing MS, creating Figures 1, 2; KP: creating outline and reviewing MS.

FUNDING

The author(s) disclosed receipt of the following financial support for the research, authorship, and/or publication of this article: This study was funded by National Institutes of Health (grant number: Z1AHD008735), by the Spanish Society of Medical Oncology Foundation (F SEOM 2015) and the PHEiPAS patient Alliance (2016).

ACKNOWLEDGMENTS

This research was supported, in part, by the Intramural Research Program of the NIH, NICHD. We would like to thank the NIH for the enormous support in patient care and research of this disease Library Writing Center for manuscript editing assistance; In addition, we wish to thank Ying Pang for reviewing the *IRP1* section.

- Pacak K, Jochmanova I, Prodanov T, Yang C, Merino MJ, Fojo T, et al. New syndrome of paraganglioma and somatostatinoma associated with polycythemia. *J Clin Oncol*. (2013) 31:1690–8. doi: 10.1200/JCO.2012.47.1912
- Zhuang Z, Yang C, Lorenzo F, Merino M, Fojo T, Kebebew E, et al. Somatic HIF2A gain-of-function mutations in paraganglioma with polycythemia. *N Engl J Med*. (2012) 367:922–30. doi: 10.1056/NEJMoa1205119
- Castro-Vega LJ, Buffet A, De Cubas AA, Cascón A, Menara M, Khalifa E, et al. Germline mutations in FH confer predisposition to malignant pheochromocytomas and paragangliomas. *Hum Mol Genet*. (2014) 23:2440–6. doi: 10.1093/hmg/ddt639
- Crona J, Delgado Verdugo A, Maharjan R, Stålberg P, Granberg D, Hellman P, et al. Somatic mutations in H-RAS in sporadic pheochromocytoma and paraganglioma identified by exome sequencing. *J Clin Endocrinol Metab*. (2013) 98:E1266–71. doi: 10.1210/jc.2012-4257
- Yang C, Zhuang Z, Flidner SM, Shankavaram U, Sun MG, Bullova P, et al. Germ-line PHD1 and PHD2 mutations detected in patients with pheochromocytoma/paraganglioma-polycythemia. *J Mol Med*. (2015) 93:93–104. doi: 10.1007/s00109-014-1205-7
- Cascón A, Comino-Méndez I, Currás-Freixes M, de Cubas AA, Contreras L, Richter S, et al. Whole-exome sequencing identifies MDH2 as a new familial paraganglioma gene. *J Natl Cancer Inst*. (2015) 107:djv053. doi: 10.1093/jnci/djv053
- Comino-Méndez I, Tejera ÁM, Currás-Freixes M, Remacha L, Gonzalvo P, Tonda R, et al. ATRX driver mutation in a composite malignant pheochromocytoma. *Cancer Genet*. (2016) 209:272–7. doi: 10.1016/j.cancergen.2016.04.058
- Fishbein L, Leshchiner I, Walter V, Danilova L, Robertson AG, Johnson AR, et al. Comprehensive molecular characterization of

- pheochromocytoma and paraganglioma. *Cancer Cell* (2017) 31:181–93. doi: 10.1016/j.ccell.2017.01.001
16. Pang Y, Lu Y, Caisova V, Liu Y, Bullova P, Huynh TT, et al. Targeting NAD(+)/PARP DNA repair pathway as a novel therapeutic approach to SDHB-mutated cluster I pheochromocytoma and paraganglioma. *Clin Cancer Res.* (2018) 24:3423–32. doi: 10.1158/1078-0432.CCR-17-3406
 17. Carney JA. Carney triad: a syndrome featuring paraganglionic, adrenocortical, and possibly other endocrine tumors. *J Clin Endocrinol Metab.* (2009) 94:3656–62. doi: 10.1210/jc.2009-1156
 18. Buffet A, Smati S, Mansuy L, Ménara M, Lebras M, Heymann MF., et al. Mosaicism in HIF2A-related polycythemia-paraganglioma syndrome. *J Clin Endocrinol Metab.* (2014) 99:E369–73. doi: 10.1210/jc.2013-2600
 19. Castelblanco E, Santacana M, Valls J, de Cubas A, Cascón A, Robledo M, et al. Usefulness of negative and weak-diffuse pattern of SDHB immunostaining in assessment of SDH mutations in paragangliomas and pheochromocytomas. *Endocr Pathol.* (2013) 24:199–205. doi: 10.1007/s12022-013-9269-4
 20. Menara M, Oudijk L, Badoual C, Bertherat J, Lepoutre-Lussey C, Amar L, et al. SDHD immunohistochemistry: a new tool to validate SDHx mutations in pheochromocytoma/paraganglioma. *J Clin Endocrinol Metab.* (2015) 100:E287–91. doi: 10.1210/jc.2014-1870
 21. Pai R, Manipadam MT, Singh P, Ebenazer A, Samuel P, Rajaratnam S. Usefulness of Succinate dehydrogenase B (SDHB) immunohistochemistry in guiding mutational screening among patients with pheochromocytoma-paraganglioma syndromes. *APMIS* (2014) 122:1130–5. doi: 10.1111/apm.12269
 22. Santi R, Rapizzi E, Canu L, Ercolino T, Baroni G, Fucci R, et al. Potential pitfalls of SDH immunohistochemical detection in paragangliomas and pheochromocytomas harbouring germline SDHx gene mutation. *Anticancer Res.* (2017) 37:805–12. doi: 10.21873/anticancer.11381
 23. Tomlinson IP, Alam NA, Rowan AJ, Barclay E, Jaeger EE, Kelsell D., et al. Germline mutations in FH predispose to dominantly inherited uterine fibroids, skin leiomyomata and papillary renal cell cancer. *Nat Genet.* (2002) 30:406–10. doi: 10.1038/ng849
 24. Gupta G, Pacak K, Committee AAS. Precision medicine: an update on genotype/biochemical phenotype relationships in pheochromocytoma/paraganglioma patients. *Endocr Pract.* (2017) 23:690–704. doi: 10.4158/EP161718.RA
 25. Clark GR, Sciacovelli M, Gaude E, Walsh DM, Kirby G, Simpson MA., et al. Germline FH mutations presenting with pheochromocytoma. *J Clin Endocrinol Metab.* (2014) 99:E2046–50. doi: 10.1210/jc.2014-1659
 26. Yang C, Sun MG, Matro J, Huynh TT, Rahimpour S, Prchal JT., et al. Novel HIF2A mutations disrupt oxygen sensing, leading to polycythemia, paragangliomas, and somatostatinomas. *Blood* (2013) 121:2563–6. doi: 10.1182/blood-2012-10-460972
 27. Adari H, Lowy DR, Willumsen BM, Der CJ, McCormick F. Guanosine triphosphatase activating protein (GAP) interacts with the p21 ras effector binding domain. *Science* (1988) 240:518–21. doi: 10.1126/science.2833817
 28. Toledo RA, Qin Y, Cheng ZM, Gao Q, Iwata S, Silva GM, et al. Recurrent mutations of chromatin-remodeling genes and kinase receptors in pheochromocytomas and paragangliomas. *Clin Cancer Res.* (2016) 22:2301–10. doi: 10.1158/1078-0432.CCR-15-1841
 29. Fishbein L, Khare S, Wubbenhorst B, DeSloover D, D'Andrea K, Merrill S., et al. Whole-exome sequencing identifies somatic ATRX mutations in pheochromocytomas and paragangliomas. *Nat Commun.* (2015) 6:6140. doi: 10.1038/ncomms7140
 30. Pang Y, Gupta G, Yang C, Wang H, Huynh TT, Abdullaev Z, et al. A novel splicing site IRP1 somatic mutation in a patient with pheochromocytoma and JAK2(V617F) positive polycythemia vera: a case report. *BMC Cancer* (2018) 18:286. doi: 10.1186/s12885-018-4127-x
 31. Pollard PJ, Brière JJ, Alam NA, Barwell J, Barclay E, Wortham NC, et al. Accumulation of Krebs cycle intermediates and over-expression of HIF1alpha in tumours which result from germline FH and SDH mutations. *Hum Mol Genet.* (2005) 14:2231–9. doi: 10.1093/hmg/ddi227
 32. Dahia PL. Pheochromocytoma and paraganglioma pathogenesis: learning from genetic heterogeneity. *Nat Rev Cancer.* (2014) 14:108–19. doi: 10.1038/nrc3648
 33. Isaacs JS, Jung YJ, Mole DR, Lee S, Torres-Cabala C, Chung YL., et al. HIF overexpression correlates with biallelic loss of fumarate hydratase in renal cancer: novel role of fumarate in regulation of HIF stability. *Cancer Cell* (2005) 8:143–53. doi: 10.1016/j.ccr.2005.06.017
 34. Clark GR, Sciacovelli M, Gaude E, Walsh DM, Kirby G, Simpson MA., et al. Germline FH mutations presenting with pheochromocytoma. *J Clin Endocrinol Metab.* (2014) 99:E2046–50. doi: 10.1210/jc.2014-1659
 35. Tian H, McKnight SL, Russell DW. Endothelial PAS domain protein 1 (EPAS1), a transcription factor selectively expressed in endothelial cells. *Genes Dev.* (1997) 11:72–82. doi: 10.1101/gad.11.1.72
 36. Lorenzo FR, Yang C, Ng Tang Fui M, Vankayalapati H, Zhuang Z, Huynh T, et al. A novel EPAS1/HIF2A germline mutation in a congenital polycythemia with paraganglioma. *J Mol Med.* (2013) 91:507–12. doi: 10.1007/s00109-012-0967-z
 37. Därr R, Nambuba J, Del Rivero J, Janssen I, Merino M, Todorovic M, et al. Novel insights into the polycythemia-paraganglioma-somatostatinoma syndrome. *Endocr Relat Cancer* (2016) 23:899–908. doi: 10.1530/ERC-16-0231
 38. Pacak K, Chew EY, Pappo AS, Yang C, Lorenzo FR, Wilson MW., et al. Ocular manifestations of hypoxia-inducible factor-2alpha paraganglioma-somatostatinoma-polycythemia syndrome. *Ophthalmology* (2014) 121:2291–3. doi: 10.1016/j.ophtha.2014.06.019
 39. Mihailovich M, Militti C, Gabaldón T, Gebauer F. Eukaryotic cold shock domain proteins: highly versatile regulators of gene expression. *BioEssays* (2010) 32:109–18. doi: 10.1002/bies.200900122
 40. Kobayashi H, Kawachi D, Hashimoto Y, Ogata T, Murakami F. The control of precerebellar neuron migration by RNA-binding protein Csd1. *Neuroscience* (2013) 253:292–303. doi: 10.1016/j.neuroscience.2013.08.055
 41. Cerami E, Gao J, Dogrusoz U, Gross BE, Sumer SO, Aksoy BA, et al. The cBio cancer genomics portal: an open platform for exploring multidimensional cancer genomics data. *Cancer Discovery* (2012) 2:401–4. doi: 10.1158/2159-8290.CD-12-0095
 42. Dormoy-Raclet V, Markovits J, Malato Y, Huet S, Lagarde P, Montaudon D, et al. Unr, a cytoplasmic RNA-binding protein with cold-shock domains, is involved in control of apoptosis in ES and HuH7 cells. *Oncogene* (2007) 26:2595–605. doi: 10.1038/sj.onc.1210068
 43. Elatmani H, Dormoy-Raclet V, Dubus P, Dautry F, Chazaud C, Jacquemin-Sablon H. The RNA-binding protein Unr prevents mouse embryonic stem cells differentiation toward the primitive endoderm lineage. *Stem Cells* (2011) 29:1504–16. doi: 10.1002/stem.712
 44. Enlund F, Behboudi A, Andrén Y, Oberg C, Lendahl U, Mark J, et al. Altered notch signaling resulting from expression of a WAMTP1-MAML2 gene fusion in mucoepidermoid carcinomas and benign Warthin's tumors. *Exp Cell Res.* (2004) 292:21–8. doi: 10.1016/j.yexcr.2003.09.007
 45. Amelio AL, Fallahi M, Schaub FX, Zhang M, Lawani MB, Alperstein AS, et al. CRTC1/MAML2 gain-of-function interactions with MYC create a gene signature predictive of cancers with CREB-MYC involvement. *Proc Natl Acad Sci USA.* (2014) 111:E3260–8. doi: 10.1073/pnas.1319176111
 46. Wang K, Singh D, Zeng Z, Coleman SJ, Huang Y, Savich GL, et al. MapSplice: accurate mapping of RNA-seq reads for splice junction discovery. *Nucleic Acids Res.* (2010) 38:e178. doi: 10.1093/nar/gkq622
 47. Wang L, Lam G, Thummel CS. Med24 and Mdh2 are required for Drosophila larval salivary gland cell death. *Dev Dyn.* (2010) 239:954–64. doi: 10.1002/dvdy.22213
 48. Letouzé E, Martinelli C, Lorient C, Burnichon N, Abermil N, Ottolenghi C, et al. SDH mutations establish a hypermethylator phenotype in paraganglioma. *Cancer Cell.* (2013) 23:739–52. doi: 10.1016/j.ccr.2013.04.018
 49. Kaelin WG Jr, Ratcliffe PJ. Oxygen sensing by metazoans: the central role of the HIF hydroxylase pathway. *Mol Cell.* (2008) 30:393–402. doi: 10.1016/j.molcel.2008.04.009
 50. Ladroue C, Carcenac R, Leporrier M, Gad S, Le Hello C, Galateau-Salle F, et al. PHD2 mutation and congenital erythrocytosis with paraganglioma. *N Engl J Med.* (2008) 359:2685–92. doi: 10.1056/NEJMoa0806277
 51. Meyron-Holtz EG, Ghosh MC, Rouault TA. Mammalian tissue oxygen levels modulate iron-regulatory protein activities *in vivo*. *Science* (2004) 306:2087–90. doi: 10.1126/science.1103786
 52. Wilkinson N, Pantopoulos K. IRP1 regulates erythropoiesis and systemic iron homeostasis by controlling HIF2alpha mRNA translation. *Blood* (2013) 122:1658–68. doi: 10.1182/blood-2013-03-492454

53. Wells D, Hoffman D, Kedes L. Unusual structure, evolutionary conservation of non-coding sequences and numerous pseudogenes characterize the human H3.3 histone multigene family. *Nucleic Acids Res.* (1987) 15:2871–89. doi: 10.1093/nar/15.7.2871
54. Lehninger BPJ. Principles of biochemistry. In: Nelson DL, editors. MCC, 4th edition. New York, NY: W. H. Freeman and Co (2004), p. 1119.
55. Khuong-Quang DA, Buczkowicz P, Rakopoulos P, Liu XY, Fontebasso AM, Bouffet E, et al. K27M mutation in histone H3.3 defines clinically and biologically distinct subgroups of pediatric diffuse intrinsic pontine gliomas. *Acta Neuropathol.* (2012) 124:439–47. doi: 10.1007/s00401-012-0998-0
56. Wu G, Broniscer A, McEachron TA, Lu C, Paugh BS, Beckfort J., et al. Somatic histone H3 alterations in pediatric diffuse intrinsic pontine gliomas and non-brainstem glioblastomas. *Nat Genet.* (2012) 44:251–3. doi: 10.1038/ng.1102
57. Behjati S, Tarpey PS, Presneau N, Scheipl S, Pillay N, Van Loo P, et al. Distinct H3F3A and H3F3B driver mutations define chondroblastoma and giant cell tumor of bone. *Nat Genet.* (2013) 45:1479–82. doi: 10.1038/ng.2814
58. Iwata S, Yonemoto T, Ishii T, Araki A, Hagiwara Y, Tatezaki SI. Multicentric giant cell tumor of bone and paraganglioma: a case report. *JBJS Case Connect.* (2013) 3:e23. doi: 10.2106/JBJS.CC.L00155
59. Rand V, Huang J, Stockwell T, Ferreira S, Buzko O, Levy S., et al. Sequence survey of receptor tyrosine kinases reveals mutations in glioblastomas. *Proc Natl Acad Sci USA.* (2005) 102:14344–9. doi: 10.1073/pnas.0507200102
60. Clynes D, Gibbons RJ. ATRX and the replication of structured DNA. *Curr Opin Genet Dev.* (2013) 23:289–94. doi: 10.1016/j.gde.2013.01.005
61. Kernohan KD, Vernimmen D, Gloor GB, Berube NG. Analysis of neonatal brain lacking ATRX or McCP2 reveals changes in nucleosome density, CTCF binding and chromatin looping. *Nucleic Acids Res.* (2014) 42:8356–68. doi: 10.1093/nar/gku564
62. Ratnakumar K, Bernstein E. ATRX: the case of a peculiar chromatin remodeler. *Epigenetics* (2013) 8:3–9. doi: 10.4161/epi.23271
63. Gibbons RJ, Picketts DJ, Villard L, Higgs DR. Mutations in a putative global transcriptional regulator cause X-linked mental retardation with alpha-thalassemia (ATR-X syndrome). *Cell* (1995) 80:837–45. doi: 10.1016/0092-8674(95)90287-2
64. Liu XY, Gerges N, Korshunov A, Sabha N, Khuong-Quang DA, Fontebasso AM, et al. Frequent ATRX mutations and loss of expression in adult diffuse astrocytic tumors carrying IDH1/IDH2 and TP53 mutations. *Acta Neuropathol.* (2012) 124:615–25. doi: 10.1007/s00401-012-1031-3
65. Persky MS, Setton A, Niimi Y, Hartman J, Frank D, Berenstein A. Combined endovascular and surgical treatment of head and neck paragangliomas—a team approach. *Head Neck.* (2002) 24:423–31. doi: 10.1002/hed.10068
66. Eisenhofer G, Lenders JW, Goldstein DS, Mannelli M, Csako G, Walther MM, et al. Pheochromocytoma catecholamine phenotypes and prediction of tumor size and location by use of plasma free metanephrines. *Clin Chem.* (2005) 51:735–44. doi: 10.1373/clinchem.2004.045484
67. van der Harst E, de Herder WW, de Krijger RR, Bruining HA, Bonjer HJ, Lamberts SW, et al. The value of plasma markers for the clinical behaviour of pheochromocytomas. *Eur J Endocrinol.* (2002) 147:85–94. doi: 10.1530/eje.0.1470085
68. Pacak K. Pheochromocytoma: a catecholamine and oxidative stress disorder. *Endocr Regul.* (2011) 45:65–90. doi: 10.4149/endo_2011_02_65
69. Zuber SM, Kantorovich V, Pacak K. Hypertension in pheochromocytoma: characteristics and treatment. *Endocrinol Metab Clin North Am.* (2011) 40:295–311, vii. doi: 10.1016/j.ecl.2011.02.002
70. Eisenhofer G, Pacak K, Huynh TT, Qin N, Bratslavsky G, Linehan WM., et al. Catecholamine metabolomic and secretory phenotypes in pheochromocytoma. *Endocr Relat Cancer.* (2011) 18:97–111. doi: 10.1677/ERC-10-0211
71. Huynh TT, Pacak K, Wong DL, Linehan WM, Goldstein DS, Elkhoulou AG, et al. Transcriptional regulation of phenylethanolamine N-methyltransferase in pheochromocytomas from patients with von Hippel-Lindau syndrome and multiple endocrine neoplasia type 2. *Ann NY Acad Sci.* (2006) 1073:241–52. doi: 10.1196/annals.1353.026
72. Nilsson H, Jögi A, Beckman S, Harris AL, Poellinger L, Pahlman S. HIF-2 α expression in human fetal paraganglia and neuroblastoma: relation to sympathetic differentiation, glucose deficiency, and hypoxia. *Exp Cell Res.* (2005) 303:447–56. doi: 10.1016/j.yexcr.2004.10.003
73. Pacak K, Eisenhofer G. An assessment of biochemical tests for the diagnosis of pheochromocytoma. *Nat Clin Pract Endocrinol Metab.* (2007) 3:744–5. doi: 10.1038/ncpendmet0615
74. Ito Y, Fujimoto Y, Obara T. The role of epinephrine, norepinephrine, and dopamine in blood pressure disturbances in patients with pheochromocytoma. *World J Surg.* (1992) 16:759–63; discussion. 763–754.
75. Pacak K, Eisenhofer G, Ilias I. Diagnosis of pheochromocytoma with special emphasis on MEN2 syndrome. *Hormones* (2009) 8:111–6. doi: 10.14310/horm.2002.1227
76. Van Der Horst-Schrivers AN, Osinga TE, Kema IP, Van Der Laan BF, Dullaart RP. Dopamine excess in patients with head and neck paragangliomas. *Anticancer Res.* (2010) 30:5153–58.
77. Righini Ch, Pecher M, Halimi S, Magne JL, Rey E. [Malignant carotid paraganglioma. A case report]. *Ann Otolaryngol Chir Cervicofac.* (2003) 120:103–8.
78. van Duinen N, Corssmit EP, de Jong WH, Brookman D, Kema IP, Romijn JA. Plasma levels of free metanephrines and 3-methoxytyramine indicate a higher number of biochemically active HNPGL than 24-h urinary excretion rates of catecholamines and metabolites. *Eur J Endocrinol.* (2013) 169:377–82. doi: 10.1530/EJE-13-0529
79. Goldberg LI. Cardiovascular and renal actions of dopamine: potential clinical applications. *Pharmacol Rev.* (1972) 24:1–29.
80. Marmon LM, Albrecht F, Canessa LM, Hoy GR, Jose PA. Identification of dopamine 1A receptors in the rat small intestine. *J Surg Res.* (1993) 54:616–20. doi: 10.1006/jsre.1993.1094
81. Shen WW. Vomiting, chemoreceptor trigger zone, and dopamine. *Psychosomatics* (1989) 30:118–9. doi: 10.1016/S0033-3182(89)72333-1
82. Eisenhofer G, Lenders JW, Timmers H, Mannelli M, Grebe SK, Hofbauer LC, et al. Measurements of plasma methoxytyramine, normetanephrine, and metanephrine as discriminators of different hereditary forms of pheochromocytoma. *Clin Chem.* (2011) 57:411–20. doi: 10.1373/clinchem.2010.153320
83. Lenders JW, Duh QY, Eisenhofer G, Gimenez-Roqueplo AP, Grebe SK, Murad MH, et al. Pheochromocytoma and paraganglioma: an endocrine society clinical practice guideline. *J Clin Endocrinol Metab.* (2014) 99:1915–42. doi: 10.1210/jc.2014-1498
84. Därr R, Kuhn M, Bode C, Bornstein SR, Pacak K, Lenders JWM., et al. Accuracy of recommended sampling and assay methods for the determination of plasma-free and urinary fractionated metanephrines in the diagnosis of pheochromocytoma and paraganglioma: a systematic review. *Endocrine* (2017) 56:495–503. doi: 10.1007/s12020-017-1300-y
85. Weise M, Merke DP, Pacak K, Walther MM, Eisenhofer G. Utility of plasma free metanephrines for detecting childhood pheochromocytoma. *J Clin Endocrinol Metab.* (2002) 87:1955–60. doi: 10.1210/jcem.87.5.8446
86. Eisenhofer G, Peitzsch M, McWhinney BC. Impact of LC-MS/MS on the laboratory diagnosis of catecholamine-producing tumors. *TrAC Trends in Anal Chem.* (2016) 84:106–16. doi: 10.1016/j.trac.2016.01.027
87. Ilias I, Pacak K. Current approaches and recommended algorithm for the diagnostic localization of pheochromocytoma. *J Clin Endocrinol Metab.* (2004) 89:479–91. doi: 10.1210/jc.2003-031091
88. Pacak K, Ilias I, Adams KT, Eisenhofer G. Biochemical diagnosis, localization and management of pheochromocytoma: focus on multiple endocrine neoplasia type 2 in relation to other hereditary syndromes and sporadic forms of the tumour. *J Intern Med.* (2005) 257:60–8. doi: 10.1111/j.1365-2796.2004.01425.x
89. Archier A, Varoquaux A, Garrigue P, Montava M, Guerin C, Gabriel S., et al. Prospective comparison of (68)Ga-DOTATATE and (18)F-FDOPA PET/CT in patients with various pheochromocytomas and paragangliomas with emphasis on sporadic cases. *Eur J Nucl Med Mol Imaging* (2016) 43:1248–57. doi: 10.1007/s00259-015-3268-2
90. Garrigue P, Bodin-Hullin A, Balasse L, et al. The Evolving Role of Succinate in Tumor Metabolism: An (18)F-FDG-Based Study. *J Nucl Med.* (2017) 58:1749–55. doi: 10.2967/jnumed.117.192674
91. Taieb D, Hicks RJ, Pacak K. PET Imaging for endocrine malignancies: from woe to go. *J Nucl Med.* (2017) 58:878–80. doi: 10.2967/jnumed.117.189688
92. Schiesser M, Veit-Haibach P, Muller MK, Weber M, Bauerfeind P, Hany T, et al. Value of combined 6-[18F]fluorodihydroxyphenylalanine PET/CT

- for imaging of neuroendocrine tumours. *Br J Surg.* (2010) 97:691–97. doi: 10.1002/bjs.6937
93. Sagman U, Mullen JB, Kovacs K, Kerbel R, Ginsberg R, Reubi JC. Identification of somatostatin receptors in human small cell lung carcinoma. *Cancer* (1990) 66:2129–33. doi: 10.1002/1097-0142(19901115)66:10<2129::AID-CNCR2820661015>3.0.CO;2-T
 94. Janssen I, Blanchet EM, Adams K, Chen CC, Millo CM, Herscovitch P, et al. Superiority of [68Ga]-DOTATATE PET/CT to other functional imaging modalities in the localization of SDHB-associated metastatic pheochromocytoma and paraganglioma. *Clin Cancer Res.* (2015) 21:3888–95. doi: 10.1158/1078-0432.CCR-14-2751
 95. Janssen I, Chen CC, Millo CM, Ling A, Taieb D, Lin FI., et al. PET/CT comparing (68)Ga-DOTATATE and other radiopharmaceuticals and in comparison with CT/MRI for the localization of sporadic metastatic pheochromocytoma and paraganglioma. *Eur J Nucl Med Mol Imaging* (2016) 43:1784–91. doi: 10.1007/s00259-016-3357-x
 96. Janssen I, Chen CC, Taieb D, Patronas NJ, Millo CM, Adams KT, et al. 68Ga-DOTATATE PET/CT in the localization of head and neck paragangliomas compared with other functional imaging modalities and CT/MRI. *J Nucl Med.* (2016) 57:186–91. doi: 10.2967/jnumed.115.161018
 97. Janssen I, Chen CC, Zhuang Z, Millo CM, Wolf KI, Ling A, et al. Functional imaging signature of patients presenting with polycythemia/paraganglioma syndromes. *J Nucl Med.* (2017) 58:1236–42. doi: 10.2967/jnumed.116.187690
 98. Nambuba J, Därr R, Janssen I, Bullova P, Adams KT, Millo C, et al. Functional imaging experience in a germline fumarate hydratase mutation-positive a patient with pheochromocytoma and paraganglioma. *AACE Clin Case Rep Summer* (2016) 2:e176–81. doi: 10.4158/EP15759.CR
 99. Taieb D, Jha A, Guerin C, Pang Y, Adams KT, Chen CC, et al. 18F-FDOPA PET/CT imaging of MAX-related pheochromocytoma. *J Clin Endocrinol Metab.* (2018) 103:1574–82. doi: 10.1210/jc.2017-02324
 100. Jha A, Ling A, Millo C, Gupta G, Viana B, Lin FI, et al. Superiority of (68)Ga-DOTATATE over (18)F-FDG and anatomic imaging in the detection of succinate dehydrogenase mutation (SDHx)-related pheochromocytoma and paraganglioma in the pediatric population. *Eur J Nucl Med Mol Imaging* (2018) 45:787–97. doi: 10.1007/s00259-017-3896-9
 101. Babic B, Patel D, Aufforth R, Assadipour Y, Sadowski SM, Quezado M, et al. Pediatric patients with pheochromocytoma and paraganglioma should have routine preoperative genetic testing for common susceptibility genes in addition to imaging to detect extra-adrenal and metastatic tumors. *Surgery* (2017) 161:220–7. doi: 10.1016/j.surg.2016.05.059
 102. Strosberg J, Krenning E. 177Lu-dotatate for midgut neuroendocrine tumors. *N Engl J Med.* (2017) 376:1391–2. doi: 10.1056/NEJMoa1607427
 103. Zovato S, Kumanova A, Demattè S, Sansovini M, Bodei L, Di Sarra D, et al. Peptide receptor radionuclide therapy (PRRT) with 177Lu-DOTATATE in individuals with neck or mediastinal paraganglioma (PGL). *Horm Metab Res.* (2012) 44:411–4. doi: 10.1055/s-0032-1311637
 104. Puranik AD, Kulkarni HR, Singh A, Baum RP. Peptide receptor radionuclide therapy with (90)Y/ (177)Lu-labelled peptides for inoperable head and neck paragangliomas (glomus tumours). *Eur J Nucl Med Mol Imaging* (2015) 42:1223–30. doi: 10.1007/s00259-015-3029-2
 105. Kong G, Grozinsky-Glasberg S, Hofman MS, et al. Efficacy of Peptide Receptor Radionuclide Therapy (PRRT) for Functional Metastatic Paraganglioma and Pheochromocytoma. *J Clin Endocrinol Metab.* (2017) 102:3278–87. doi: 10.1210/jc.2017-00816
 106. Nastos K, Cheung VTF, Toumpanakis C, Navalkisoor S, Quigley AM, Caplin M, et al. Peptide receptor radionuclide treatment and (131)I-MIBG in the management of patients with metastatic/progressive pheochromocytomas and paragangliomas. *J Surg Oncol.* (2017) 115:425–34. doi: 10.1002/jso.24553
 107. Ginj M, Zhang H, Waser B, Cescato R, Wild D, Wang X., et al. Radiolabeled somatostatin receptor antagonists are preferable to agonists for in vivo peptide receptor targeting of tumors. *Proc Natl Acad Sci USA.* (2006) 103:16436–41. doi: 10.1073/pnas.0607761103
 108. Wild D, Mäcke HR, Waser B, Reubi JC, Ginj M, Rasch H, et al. 68Ga-DOTANOC: a first compound for PET imaging with high affinity for somatostatin receptor subtypes 2 and 5. *Eur J Nucl Med Mol Imaging* (2005) 32:724. doi: 10.1007/s00259-004-1697-4
 109. Fani M, Braun F, Waser B, Beetschen K, Cescato R, Erchegyi J, et al. Unexpected sensitivity of sst2 antagonists to N-terminal radiometal modifications. *J Nucl Med.* (2012) 53:1481–9. doi: 10.2967/jnumed.112.102764
 110. Dalm SU, Nonnekens J, Doeswijk GN, de Blois E, van Gent DC, Konijnenberg MW, et al. Comparison of the therapeutic response to treatment with a 177Lu-labeled somatostatin receptor agonist and antagonist in preclinical models. *J Nucl Med.* (2016) 57:260–5. doi: 10.2967/jnumed.115.167007
 111. Nicolas GP, Mansi R, McDougall L, Kaufmann J, Bouterfa H, Wild D, et al. Biodistribution, pharmacokinetics, and dosimetry of (177)Lu-, (90)Y-, and (111)In-labeled somatostatin receptor antagonist OPS201 in comparison to the agonist (177)Lu-dotatate: the mass effect. *J Nucl Med.* (2017) 58:1435–41. doi: 10.2967/jnumed.117.191684
 112. Reubi JC, Waser B, Macke H, Rivier J. Highly increased 125I-JR11 antagonist binding *in vitro* reveals novel indications for sst2 targeting in human cancers. *J Nucl Med.* (2017) 58:300–6. doi: 10.2967/jnumed.116.177733

Conflict of Interest Statement: The authors declare that the research was conducted in the absence of any commercial or financial relationships that could be construed as a potential conflict of interest.

Copyright © 2018 Alrezk, Suarez, Tena and Pacak. This is an open-access article distributed under the terms of the Creative Commons Attribution License (CC BY). The use, distribution or reproduction in other forums is permitted, provided the original author(s) and the copyright owner(s) are credited and that the original publication in this journal is cited, in accordance with accepted academic practice. No use, distribution or reproduction is permitted which does not comply with these terms.